DESIGN AND RESULTS OF A TIME RESOLVED SPECTROMETER FOR THE 5 MeV PHOTO-INJECTOR PHIN

D. Egger, O. Mete, EPFL, Lausanne, Switzerland & CERN, Geneva, Switzerland

A. Dabrowski, S. Doebert and T. Lefèvre, CERN, Geneva, Switzerland

Abstract

The CLIC Test Facility 3 (CTF3) drive beam injector should provide high intensity and high quality electron beams. The present installation relies on a thermionic gun followed by a complex RF bunching system. As an upgrade to improve the beam emittance and the energy spread and to minimize the beam losses, a photo-injector is being developed and tested at CERN. One of the major challenges is to provide a 3.5A beam with a stable (0.1%) beam energy over 1.2 μs and a relative energy spread smaller than 1%. A 90° spectrometer line consisting of a segmented dump and an Optical Transition Radiation screen has been built in order to study these issues. The following paper describes its design and shows performances during the beam commissioning.

THE PHIN PHOTO-INJECTOR

The CTF3 drive beam injector is a key part of the accelerator, driving the performance of the whole complex. It must provide high intensity (3.5A) 1.2 μs long electron pulses, bunched at 1.5 GHz. Since the CTF3 linac is designed to work with fully loaded acceleration [1], intensity fluctuations translate in energy fluctuations, which must be kept below 0.1%.

In the current CTF3 injector, electrons are created using a thermionic gun [2]. The RF manipulations are done using a 1.5 GHz sub-harmonic bunching system, with the required phase coding capabilities [3] following by a 3 GHz bunching system which is inefficient, creating losses of up to (30%) and remaining satellites bunches at 3GHz (8%).

Photo-injectors have the potential to overcome most of these limitations. The electrons are created directly as bunches and the bunch length and the phase coding can be controlled by the laser system. A collaboration between LAL, CCLRC and CERN has been setup to develop and commission a photo-injector for CTF3, named PHIN [4]. The electrons exit the gun with a 5.5 MeV nominal energy. The laser pulse length and energy is tuned to generate 8 ps long electron bunches with a charge of 2.33 nC [4, 5]. The beam line is equipped with several diagnostics to measure the emittance, charge and energy [6]. This paper describes the characteristics of the PHIN spectrometer line and presents its performance obtained during the first commissioning phase.
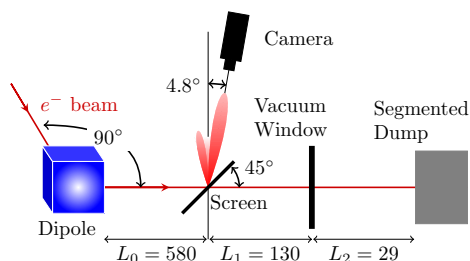

Figure 1: Layout (in mm) of the PHIN spectrometer.

SPECTROMETER DESIGN

The PHIN spectrometer consists of a dipole magnet, an Optical Transition Radiation (OTR) screen coupled to a gated intensified camera to precisely measure the beam energy and its energy spread and a segmented dump to provide time resolved measurements, see Fig. 1. The dipole bends the electron beam by 90°, and induces a dispersion of $D_{OTR} = 820.2$ mm and 1067 mm at the respective positions of the OTR screen and the segmented dump. Located at a distance of 580 mm from the exit of the dipole magnet, the OTR screen [7] is made of a thin aluminum foil, tilted by 45° with respect to the beam trajectory. The photons, emitted in the top vertical direction, are captured by an intensified camera. Figure 2 shows the expected OTR intensity distribution at the position of the camera. At low beam energy, the OTR lobes have a strong asymmetry and the maximum of the emitted OTR light can be found at 4.8° from the vertical axis. Therefore the camera has been placed at this angle, which maximize the light intensity seen by the camera.
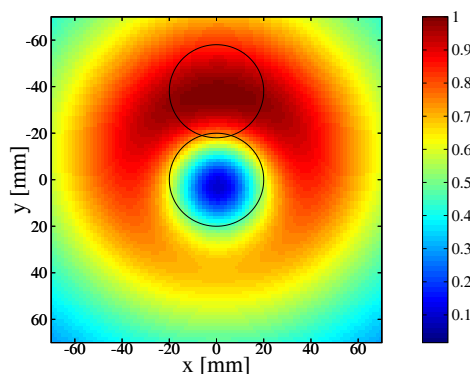

Figure 2: Relative OTR intensity produced by a 5.5 MeV e^- beam at the camera plane.

Table 1: Percent of beam stopped and mean range of electrons for the considered materials.

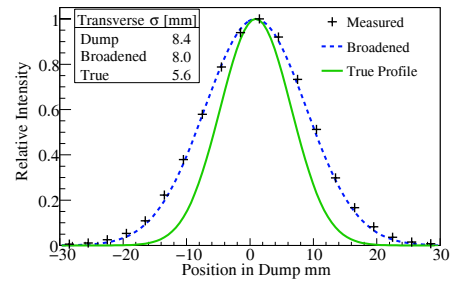| material	beam stopped [%]	< range > [cm]
Al	98.6	1.25
Fe	94.5	0.46
Cu	93.9	0.42
W	82.3	0.21
Pb	80.6	0.35

Figure 3: Beam profile at the segmented dump with and without the effect of the screen and vacuum window.

Figure 4: Temperature increase in the dump.

The segmented dump is placed at the end of the beam line, outside of the vacuum chamber, at 755 mm from the dipole exit. It is made of parallel metallic plates, working as faraday cups, and by measuring the charge stopped in each plate a horizontal profile can be reconstructed [8]. The design of the detector has been performed based on Geant4 [9] simulations. A simple geometry with a single block of metal was first simulated in order to select the best material. The plate should ideally stop most of incoming particles in a reasonably short distance. Results obtained for several materials are shown in Tab. 1. With only 5.5% of particles backscattering and a mean range of 0.46 cm, iron based materials are good choices. The spatial resolution of the dump is limited by scattering processes inside the segments, where one electron entering one plate would be finally stopped in a neighboring one. At low beam energies this effect is small and with plate widths larger than 1 mm, multiple scattering is negligible. Therefore the final detector is made out of 20 plates of 2 mm thick stainless steel grade 304L spaced by 1 mm, which would provide measurements with a density of 4 channels$/\sigma$ for a 1% energy spread. The thermal load induced on such a dump by a nominal PHIN beam was found, using Geant4, to be negligible as can bee seen in Fig. 4.

More detailed simulations have been performed in a second stage taking into account all the components of the beam line, i.e. the dipole, the OTR screen, the vacuum window and the segmented dump. At low energies, the OTR screen and the vacuum window significantly increase the beam divergence translating into a broadening of the transverse beam size at the dump position. This effect is illustrated in Fig. 3, which shows the expected beam profile at the dump position with and without these elements. The beam size increases by 4 mm. In this example the beam energy spread is 0.63%. The performance of the segmented dump is nevertheless excellent with an agreement between the beam size arriving on the dump (Broadened) and the reconstructed profile (Measured) within 4%.

BEAM BASED MEASUREMENTS

A typical OTR image is presented in Fig. 5. Depending on the dipole magnetic strength, the horizontal beam position directly translates into beam energy. The measured horizontal profile has a contribution from both the natural horizontal beam size σ_b and the energy spread.
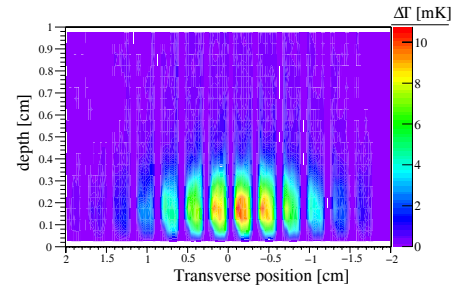
$$\sigma_{E,OTR} = \sqrt{\sigma_{meas,OTR}^2 - \sigma_{beam}^2} \qquad (1)$$

Each of the dump segments are directly connected through 50 Ohms to an 100 MSa/s analog to digital converter. The 20 channels provide thus a time resolved transverse profile. A typical 3D plot of the beam intensity as function of time and momentum is shown in Fig. 6. To extract the energy spread, $\sigma_{E,d}$, the intrinsic size of the beam must be removed, but also the beam divergence increase from the OTR screen, σ_s', and the vacuum window σ_{vac}':

$$\sigma_{E,d} = \sqrt{(\sigma_d - L_1 \tan(\sigma_s') - L_2 \tan(\sigma_{vac}'))^2 - \sigma_b^2} \qquad (2)$$

σ_b depends on the machine conditions and is given through PARMELA simulations and σ_s' and σ_{vac}' are given by Geant4 simulations.
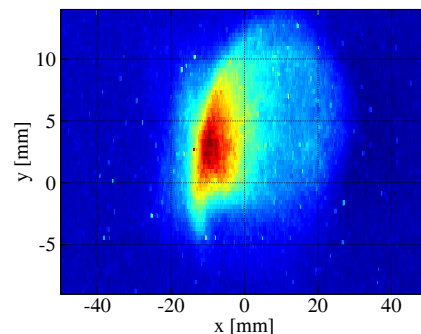

Figure 5: Beam profile from the intensified camera.
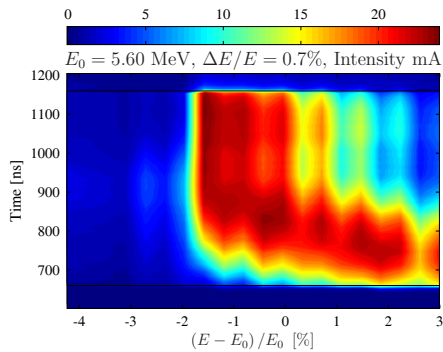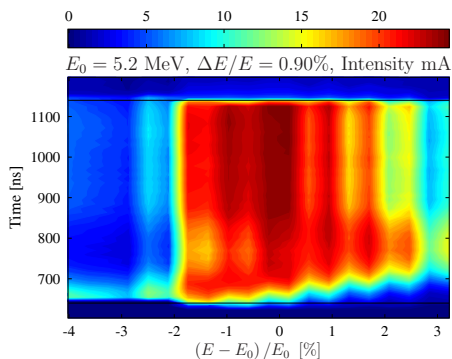
Figure 6: Beam loading in PHIN.

Figure 7: Compensated beam loading.

Beam Loading

In CTF3 the RF structures are designed to work with high beam loading, where the first particles entering a filled RF cavity are accelerated more than the following ones. This induces a strong energy variation in the first part of the pulse. One way to compensate the effect of beam loading is to shift the timing of the RF pulse relative to the beam so that the first electrons enter a partially filled gun and to shape the input RF pulse. A time resolved spectrum with high beam loading is shown in Fig. 6. A spectrum with beam loading compensated is displayed in Fig. 7. A summary of the relative mean energy for the three RF beam loading cases is shown in Fig. 8.
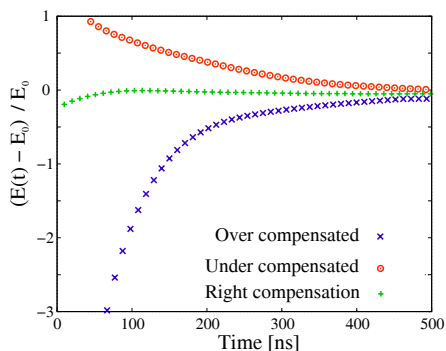

Figure 8: The measured beam relative mean time resolved energy fluctuation for different beam loading RF settings.
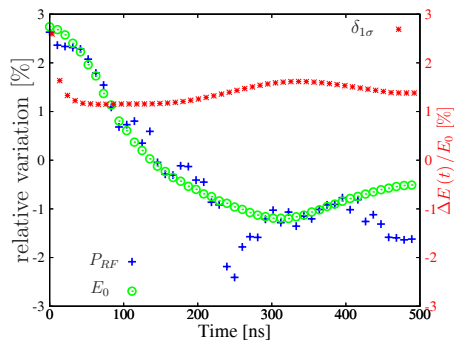
06 Beam Instrumentation and Feedback

T03 Beam Diagnostics and Instrumentation

Figure 9: Relative variation of the mean energy and RF power showing strong correlation.

RF Correlation

Energy variations along the pulse can come from fluctuations of the klystron power. As an illustration, the relative variations of the mean beam energy along the pulse are displayed in Fig. 9 (green circles) and compared to a measurement when there were RF pulse power fluctuations (blue crosses). The correlation between the two is better than 95%, showing that spectrometry can be used to study such effects.

CONCLUSION

The PHIN spectrometer has been designed to provide time resolved energy and energy spread measurements on a 5.5 MeV high intensity beam. The system has been commissioned successfully and is now routinely used as the main tool for the optimization of the RF power settings. Future work will focus on a precise study of the time resolution by comparing the measurements made with the segmented dump and the gated camera and OTR screen.

REFERENCES

[1] M. Bernard *et al.*, "First full beam loading operation with the CTF3 linac", EPAC 2004, Lucerne, Switzerland.

[2] A.Yeremian *et al.*, "CTF3 Drive-Beam Injector Design", EPAC 2002, Paris, France.

[3] P. Urschutz *et. al*, "Beam Dynamics and First Operation of the Sub-Harmonic Bunching System in the CTF3 Injector ", EPAC 2006, Edinburgh, Scotland.

[4] R. Losito *et al.*, "The PHIN Photo injector for the CTF3 Drive Beam", EPAC 2006, Edinburgh, Scotland.

[5] M. Petrarca *et al.*, "Performance of the CTF3 High Charge Photo Injector", These proceedings.

[6] T. Lefevre *et. al*, "Time Resolved Spectrometry on the CLIC Test Facility 3", EPAC 2006, Edinburgh, Scotland.

[7] K. Honkavaara, "Optical Transition Radiation in High Energy Electron Beam Diagnostics", Helsinki Institute of Physics, Internal Report, HIP-1999-04.

[8] D. Egger, *et al.*, CTF3-Note-099.

[9] S. Agostinelli *et al.*, "G4 A Simulation Toolkit", Nuclear Instruments and Methods in Physics Research Section A: Accelerators, Spectrometers, Detectors and Associated Equipment, Volume 506, Issue 3, 1 July 2003, Pages 250-303.